17th World Conference on Earthquake Engineering, 17WCEE
Sendai, Japan - September 13th to 18th 2020

DEVELOPMENT OF A NOVEL SELF-CENTERING STEEL COUPLING BEAM WITH SMA BOLTS AND ENERGY DISSIPATION DEVICES

B. Wang[1], M. Nishiyama[2], M. Tani[3], S.S. Wang[4], Y. Liu[5], S. Nagaya[6]

(1) JSPS research fellow, Department of Architecture and Architectural Engineering, Kyoto University, Kyoto, Japan, cebinwang@gmail.com
(2) Professor, Department of Architecture and Architectural Engineering, Kyoto University, Kyoto, Japan, mn@archi.kyoto-u.ac.jp
(3) Associate professor, Department of Architecture and Architectural Engineering, Kyoto University, Kyoto, Japan, tani@archi.kyoto-u.ac.jp
(4) Engineer, Berkshire Hathaway Specialty Insurance, 6111 Bollinger Canyon Rd, San Ramon, CA, USA, Shanshan.Wang@bhspecialty.com.
(5) Graduate student, Department of Architecture and Architectural Engineering, Kyoto University, Kyoto, Japan, rc.liu@archi.kyoto-u.ac.jp
(6) Graduate student, Department of Architecture and Architectural Engineering, Kyoto University, Kyoto, Japan, nagaya.shogo.37v@st.kyoto-u.ac.jp

Abstract

Coupling beam is one of the key structural components in the coupled reinforced concrete (RC) wall buildings to resist earthquake loads in high seismic zones. The primary purpose of the coupling beam is to transfer shear forces from one wall pier to the other. In the current seismic design philosophy, coupling beams are commonly designed as the first type of "sacrificial" components to dissipate earthquake energy under the strong earthquake shakings. In particular, to meet the expected seismic performance, coupling beams are typically designed and detailed to form the plastic hinges through the large inelastic responses. However, costly repair or even complete demolition caused by the significant damage in RC coupling beams is usually inevitable. The disadvantage of conventional RC coupling beams has increased the interest of the replaceable coupling beams, which can isolate the damage concentrated in the "fuse", and thus expects to be replaced after a severe earthquake. Nevertheless, significant residual deformation still exists in these components that may be difficult to replace them in practice after strong earthquakes. Therefore, seismic resilience cannot be explicitly addressed. For this reason, a novel self-centering (SC) steel coupling beam with dismountable shape memory alloy (SMA) bolts and energy dissipation devices is proposed, which can ensure damage-free behavior, SC capability, and sufficient energy dissipation capacity. This novel SC coupling beam is composed of two elastic beam segments and one rocking segment. Elastic beam segments are designed by the steel beams that connect to the RC walls at both ends of the coupling beam, whereas the rocking segment located in the middle of the coupling beam is controlled by the SMA bolts and steel angles. An ingenious shear key is designed to accommodate the rotation flexibility of the rocking segment, which can eliminate the beam elongation effect under cyclic loading. The working principle of the novel SC coupling beam was described first. Subsequently, the cyclic behavior of the SMA bolt and steel angle was investigated, which are the two core components in the SC coupling beam system. The seismic performance of the SC coupling beam was computationally investigated. Results show that the proposed SC coupling beam has excellent SC capability and sufficient energy dissipation. More importantly, the majority of the inelastic damages of this novel SC coupling beam are concentrated in the steel angles, which can be easily and rapidly inspected/replaced after earthquakes without operation disruptions. Earthquake resilience can be really achieved. The specimen exhibits the expected deformed shape under cyclic loading, where the beam elongation effect is eliminated effectively. From the design perspective, designers can cater to different performance objectives by flexibly adjusting the dimensions of the SMA bolts and steel angles. Therefore, the proposed SC coupling beam can provide a promising solution for high-performance seismic-resisting structural systems that are suitable for resilient and sustainable civil infrastructure.

Keywords: Coupling beam, Shape memory alloy, Self-centering, beam elongation, Earthquake resilience.

1. Introduction

Coupling beam is one of the key structural components in the coupled reinforced concrete (RC) wall buildings to resist earthquake loads in high seismic zones. The primary purpose of the coupling beam is to transfer shear force from one wall pier to the other. In the current seismic design philosophy, coupling beams are commonly designed as the first type of "sacrificial" components to dissipate earthquake energy under the strong earthquake shakings. In particular, to meet the expected seismic performance, coupling beams are typically designed and detailed to form the plastic hinges through the large inelastic responses. Therefore, the expected performance objectives (e.g., Life Safety and Collapse Prevention) can be achieved through such a ductile design philosophy [1, 2]. However, severe damage (e.g., concrete crushing and reinforcement buckling) accompanied by the residual (permanent) deformation of the RC coupling beams was observed in the past post-earthquake reconnaissance [3, 4]. Repair of the damage RC coupling beam is very difficult associated with disruptive and costly retrofit. The significant socio-economic losses induced by the uneconomical repair and downtime of the damaged buildings highlight the limitations of the current design concepts, which cannot meet the requirements of modern resilient and sustainable civil engineering.

The disadvantage of the conventional RC coupling beams has increased the interest of the replaceable steel coupling beams, which can isolate the damage concentrated in the fuses, and thus expects to be replaced after a severe earthquake [5-10], as shown in Fig. 1. However, it is difficult to replace them in practice if the significant residual deformation exists in these components. Therefore, seismic resilience cannot be explicitly addressed if there is absent of restoring capability in these coupling beams. In view of this problem, several types of self-centering (SC) coupling beams have been developed as high-performance structural members [11, 12]. Compared with the fat hysteretic loops with excellent energy dissipation observed in the conventional coupling beam, flag-shaped hysteretic loops with negligible residual deformation is the most significant feature of these SC coupling beams. However, the concrete located at the ends of the SC beam suffered significant damage, which is due to the large compression stresses accompanied by the beam elongation effect during the rocking behavior [11]. In addition, beam elongation may be more noticeable in the coupling beams because there are commonly designed with high beam depth. The excessive inelastic deformation induced by the beam elongation effect may compromise the SC capability of the coupling beam.

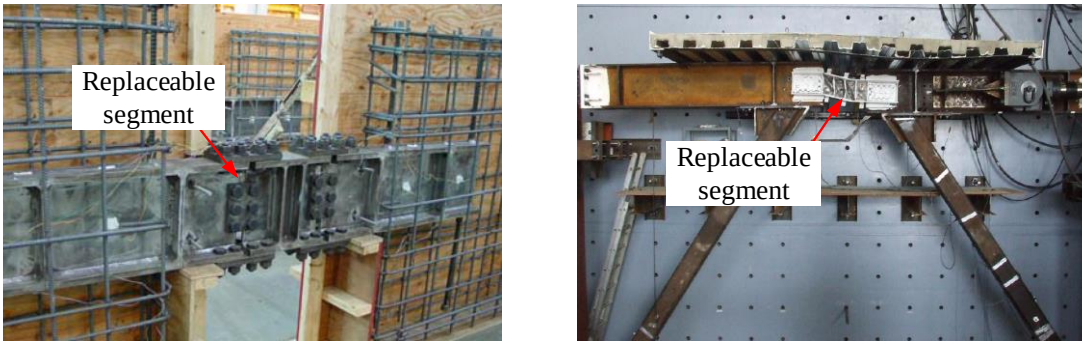

(a) (b)

Fig. 1 – Replaceable steel coupling beams: (a) Fortney et al. [5] and Mansour et al. [10].

An innovative strategy of using shape memory alloys (SMAs) as an alternative solution to achieve SC function has been proposed in the past decade. SMAs are high-performance metallic materials that can recover the initial shape through unloading due to the inherent superelastic property [13], which is particularly appealing to the community of earthquake engineering. Up to now, many innovative SMA-based devices and components have been developed and investigated in both experimental and numerical studies [14-21]. In particular, Mao et al. proposed an SMA-based coupling beam for the RC coupled wall [22]. In this concept design, an elaborately designed configuration with SMA wires as the core element was designed to undertake the shear deformation of the coupling beam. However, there are two obvious drawbacks of the

SMA wires that are the difficulty for the effective gripping and the low load-resistance capacity in seismic applications. Recently Xu et al. developed an SC link beam using posttensioned steel-SMA composite tendons [23]. Negligible residual deformation was observed even under large loading amplitude in this link beam system, but a relatively low energy dissipation was obtained because of the contribution only from the SMA bar itself. In addition, the beam elongation effect had not been considered in this system.

This paper presents a novel SC steel coupling beam for the RC coupled wall system, which can ensure damage-free behavior, SC capability, and sufficient energy dissipation capacity. This SC coupling beam obtains the high restoring force through the superelastic SMA bolts and enhances the energy dissipation by the supplemented steel angles. More importantly, the beam elongation effect observed in the conventional rocking mechanism will be eliminated by an ingenious design. In the following sections, the study starts with the structural details of this novel coupling beam. Subsequently, cyclic tests of SMA bolt and steel angles are evaluated. A numerical model of the coupling beam is developed and validated by representative test results. Finally, the seismic performance of the SC coupling beam is computationally investigated in terms of SC capability, energy dissipation, and SMA's strain.

2. SMA-based SC steel coupling beam

The configuration of the proposed SC steel coupling beam is illustrated in Fig. 2, which is composed of two non-yield segments (i.e., floor beam) and one rocking (i.e., sacrificial) segment. Two elastic segments are designed by the steel beams that connect to the adjacent RC wall piers, whereas the sacrificial segment located in the middle of the coupling beam exhibits rocking behavior. Superelastic SMA bolts are installed symmetrically at both ends of the rocking segment. As the supplemental energy dissipating device, four steel angles are connected to the elastic segments and the rocking segment through the high-strength bolts. Two shear keys are fabricated on the end plates of two elastic beams. The rocking segment is inserted in the grooves designed in the two shear keys. It is worth emphasizing that the shear key and the groove are designed with inclined surfaces. These ingenious designs are chosen to accommodate the rotation flexibility of the rocking segment, which can eliminate the beam elongation effect under cyclic loading. In this SC coupling beam system, the restoring force is provided by the superelastic SMA bolts, whereas most of contribution of energy dissipation is from the steel angles. During the earthquake shakings, all inelastic deformations will be concentrated in the SMA bolts and steel angles, which can be easily and rapidly inspected/replaced after earthquakes without operation disruptions.

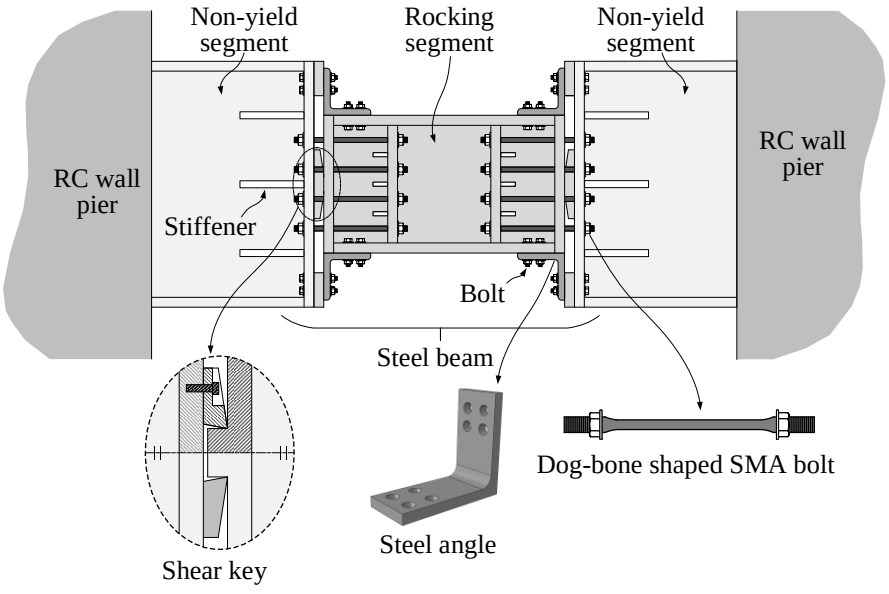

Fig. 2 – Proposed SC steel coupling beam.

3. Cyclic tests of SMA bolt and steel angles

The superelastic property of SMAs is associated with stress-induced phase transformation, which leads to strain generation during loading and strain recovery during unloading at temperatures above austenite's finish temperature A_f. Fig. 3(a) shows the schematic of SMA's mechanical behavior under uniaxial tensile loading. In the current study, the SMA bolts were machined into dog-bone shape with threads at both ends. The diameters of the threaded part and the reduced part were d_t = 8 mm and d_r = 6 mm, respectively. A satisfactory flag-shaped hysteretic loop associated with evident stress-induced phase transformation was obtained, as shown in Fig. 3(b). Detailed test results can be found in Wang et al. [20]. Furthermore, a superelastic material model in *ABAQUS* was selected to simulate the cyclic behavior of the SMA bolt. The key material parameters are as follows: Young's moduli of austenite E_A = 36.3 GPa, Young's moduli of martensite E_M = 21.0 MPa, initiation stress for forward transformation σ_{Ms} = 480.1 MPa, finishing stress for forward transformation σ_{Mf} = 630.2 MPa, starting stress for reverse transformation σ_{As} = 345.1 MPa, finishing stress for reverse transformation σ_{Af} = 170.0 MPa, Poisson's ratio of austenite ν_A = 0.33, Poisson's ratio of martensite and ν_M = 0.33, and maximum transformation strain ε_l = 2.6%. The simulated curve can predict the stress–strain relationship of the superelastic bolt reasonably well.

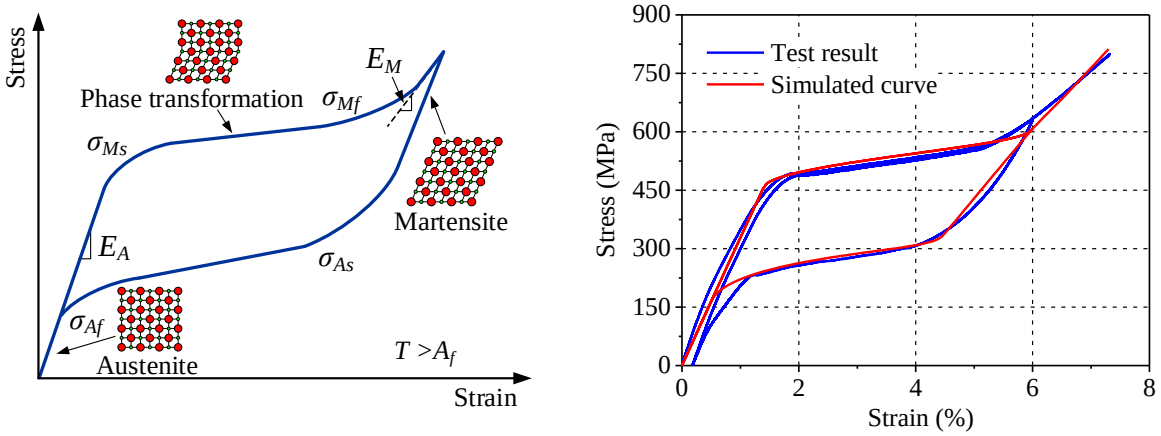

(a) (b)

Fig. 3 – Superelastic SMA: (a) mechanical behavior and (b) stress–strain relationship of an SMA bolt.

Steel angles are typically used in SC structural systems as external energy dissipation devices in recent years because of their low cost and ease of assembly and replacement [11, 24, 25]. Garlock et al. [24] concluded that steel angles can develop three plastic hinge regions in cyclic tensile loading: one hinge is near the bolt connection in the horizontal leg of the angle, whereas the two other hinges are formed on the fillet of each leg. To capture the cyclic tensile–compressive behavior of the steel angle observed in the current SC coupling beam, a special fixture that can coordinate the reversed compressive loading was designed, as shown in Fig. 4(a). The steel angles used in the current tests were made of S275 (yield strength f_y = 305.3 MPa and Young's moduli E_s = 200.0 GPa) with a cross-section of L75 × 75 × 5 mm. The specimens were designed with a gauge distance of the horizontal leg was g_c = 40 mm (l_c = 20 mm) and a gauge distance of the vertical leg was g_b = 35 mm (l_b = 15 mm), where g_c and g_b are the gages from the angle's heel to the centerline of the first row of bolt on the horizontal and vertical legs, and l_c and l_b are the gages from the edge of the stiff washer to the edge of the angle fillet on the horizontal and vertical legs, respectively. All angles were cut to a width of b = 20 mm. Fig. 4(b) presents the force–displacement relationship of the steel angles (the force is from two steel angles), which exhibited expected cyclic responses with fat hysteretic loops. During the entire loading, the angles gradually showed asymmetric force–displacement responses in the large amplitude (i.e., after 3.6 mm). This is mainly attributed to different hardening modes of the steel angle under tensile and compressive loading. In general, the simulated curves through *ABAQUS* are in good agreement with the test results. Figs. 4(c) and (d) further show the deformation shapes of the steel angles under +7.2 mm and -7.2 mm amplitude loadings, respectively.

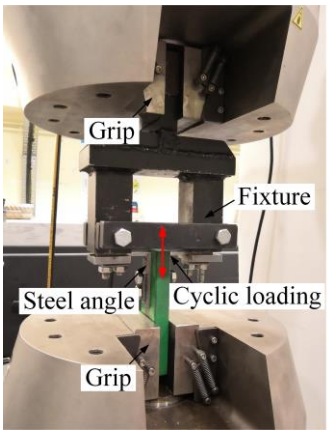

(a)

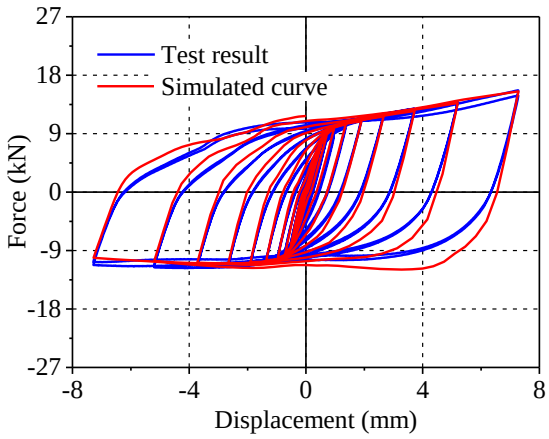

(b)

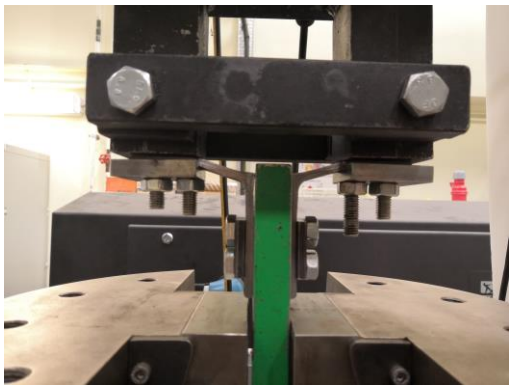

(c)

(d)

Fig. 4 – Steel angles: (a) test setup, (b) force–displacement relationships,
(c) deformation shape under +7.2 mm, and (d) deformation shape under -7.2 mm.

4. Performance evaluation of the SC steel coupling beam

4.1 Design example

The SC steel coupling beam was designed via modification of a representative steel replaceable shear link. This reference replaceable shear link was originally designed for the eccentrically braced frames (EBFs) and tested (specimen UT-3B) by Mansour et al. [10]. To ensure the replacement of the yield link after the strong earthquakes, other segments must be designed to remain essentially elastic and able to transfer the force generated by the link accounting for the strain hardening and material overstrength. Based on the value of the probable shear demand on the replaceable link, the W360 × 101 (I-shaped 356 × 254 × 10.5 × 18.7) and W610 × 372 (I-shaped 669 × 335 × 26.4 × 48) sections were selected as the yield segment and elastic beams, respectively. The specimen was fabricated by G40.21-350W grade steel (nominal yield strength f_y = 350 MPa). Apart from the SMA bolt and steel angle, the geometric dimensions and material properties of the SC steel coupling beam were the same as those of specimen UT-3B, as shown in Fig. 5.

The strain limit for the outside SMA bolts was selected as ε_{lim} = 6%. The target rotation angle of the coupling beam was determined as γ = 0.08, which was used to calculate the length of the SMA bolt L_{SMA} considering different prestrain ε_{pre} applied to the SMA bolt by $L_{SMA} \geq z_{SMA}\gamma_a/(\varepsilon_{lim} - \varepsilon_{pre})$, where z_{SMA} is the

lever arm of the outside SMA bolt. In the current design, the prestrain applied to the SMA bolts was ε_{pre} = 1% and z_{SMA} = 150 mm. Therefore, the L_{SMA} can be estimated as 240 mm. To concentrate the SMA's deformation in the reduced part and the thread parts remain elastic, the diameter of the threaded bolt was machined to d_T = 18 mm and the reduced part was d_R = 14 mm, respectively. The steel angles were designed with a section of L110 × 110 × 7 mm, in which the $g_c = g_b$ = 70 mm and $l_c = l_b$ = 39 mm, respectively.

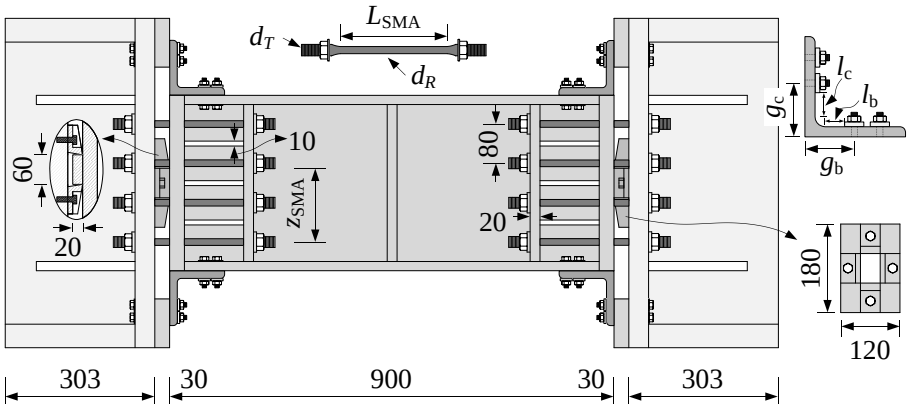

Fig. 5 – Structural details of the SC steel coupling beam (unit: mm).

4.2 Finite element analysis

Finite element analysis was carried out to understand the mechanical behavior of the SC coupling beam. A detailed three-dimensional model was developed in the finite element program *ABAQUS*, as shown in Fig. 6. All components were modeled by the 8-node solid element with reduced integration and hourglass control (C3D8R element). Different mesh strategies were used that made a balance between the accuracy of the numerical analysis and computational efficiency. "Surface-to-surface" contact was used to describe the interactions between SMA bolts and rocking segment, rocking segment and shear key, steel angle and beams, and steel angle and washer plate. To simplify the computation, "tie" constraint was defined to simulate the bolt connections. The left end of the non-yield beam was fully restrained against all translations and rotations while vertical displacements were applied to the right end. The right end was restrained against all rotations but was permitted to translate horizontal deformation.

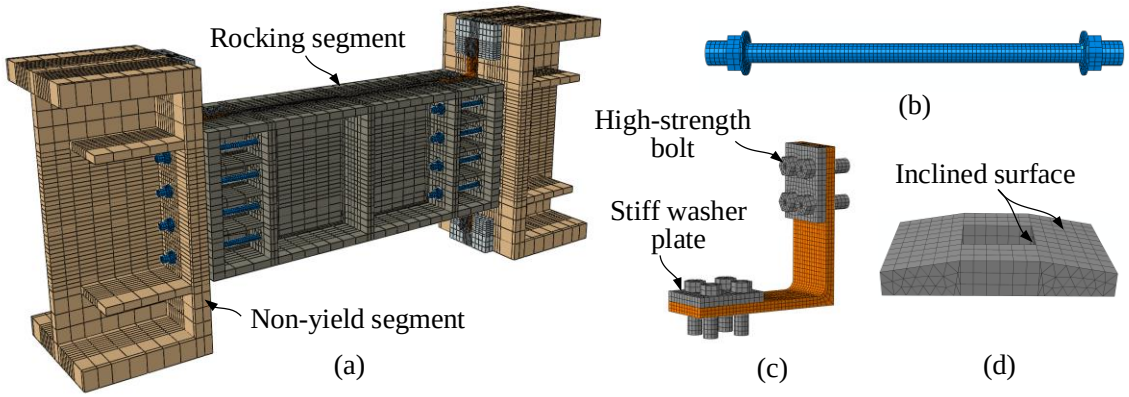

Fig. 6 – Finite element model of the SC coupling beam: (a) overview, (b) SMA bolt, (c) steel angle, and (d) shear key.

For the SMA bolts and steel angles, the validated material parameters introduced in Section 2 were used in the current analysis. For the steel bolts, a simplified bilinear kinematic hardening model in

conjunction with the von Mises yield criterion was used, wherein the yield strength was 640 MPa and the post-yield stiffness proportional to the modulus of elasticity of the steel was 1%. For the steel beams, the steel model was defined by a nonlinear combined hardening model with initial kinematic hardening modulus; C_1 = 8000 MPa, the rate factor for kinematic hardening γ_1 = 75, and the maximum changing of the yield surface Q_∞ = 110 MPa and the rate factor b = 4.

4.2 Results and discussions of cyclic responses

To validate the finite element model, numerical analysis was carried out to compare the test results reported by Mansour et al. [10] for specimen UT-3B. A modified loading protocol that consisted of one cycle of each beam rotation amplitude was implemented in the analysis to reduce the computation time. The comparison of the test and simulated hysteresis loops is shown in Fig. 7, which exhibits agreement that is satisfactory to validate the use of the numerical model as a basis for the following study. Although the conventional steel coupling beam shows fat cyclic responses with excellent energy dissipation, this type of energy dissipation mechanism is associated with permanent damage that can be difficult to repair it after the strong earthquakes. Representative deformation mode of the numerical result of UT-3B at the 0.11-rad beam rotation is presented in Fig. 8, which demonstrates very similar observation to the test result.

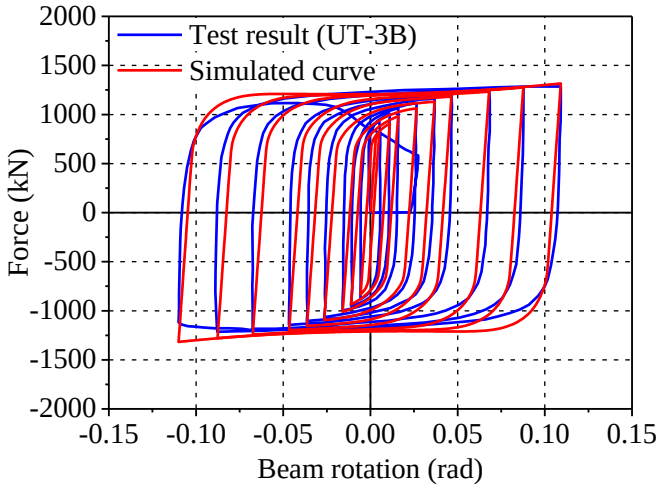

Fig. 7 – Comparison of test and simulated hysteresis loops (specimen UT-3B).

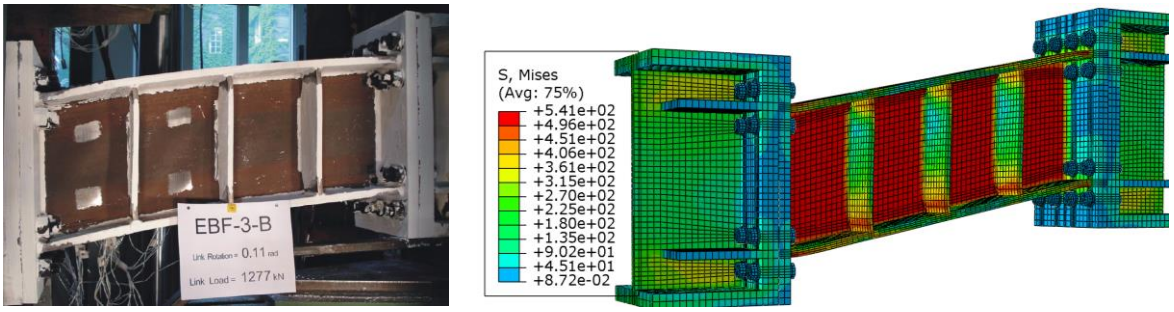

(a) (b)

Fig. 8 – Deformation shapes of specimen UT-3B: (a) test result [10] and (b) simulated result.

For the SC steel coupling beam, the loading protocol specified by the AISC [26] provision for testing EBF link-to-column connections was adapted to the current analysis. The rotation of the coupling beam increased from 0.0035, 0.005, 0.0075, 0.01, to 0.015 rad with two repeated cycles. The increment was 0.01

rad from 0.02-rad beam rotation with one cycle. The loading was finished at the target rotation of 0.08 rad. Fig. 9 shows the typical deformed shapes of the SC coupling beam subjected to + 0.08-rad loading and + 0.08-rad loading, respectively. The specimen exhibited the expected deformed shape, where the ingeniously designed shear keys can accommodate the rotation flexibility of the rocking segment, and thus eliminate the beam elongation effect under cyclic loading. In addition, the most inelastic deformation of the SC coupling beam concentrated in the SMA bolts and steel angles, whereas the rocking segment and floor beams were kept elastic.

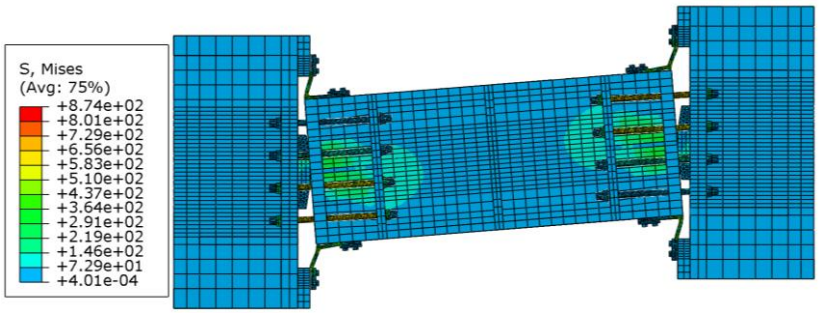

(a)

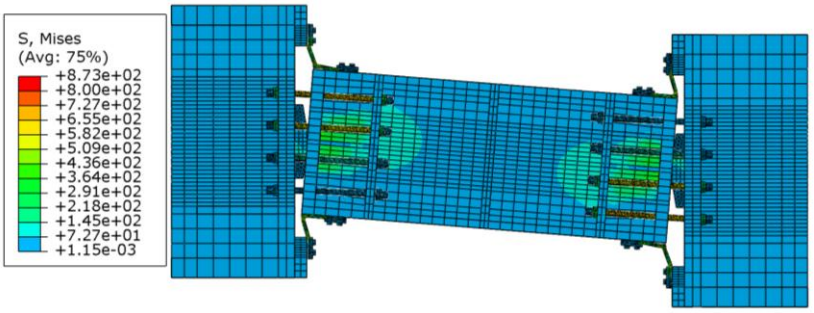

(b)

Fig. 9 – Deformation shapes of SC steel coupling beam: (a) + 0.08-rad loading and (b) - 0.08-rad loading.

Fig. 10(a) shows the force–beam rotation hysteresis loops of the SC coupling beam, which exhibited satisfactory flag-shaped responses with minor residual deformation. This is mostly due to the function of the superelastic SMA bolts designed in the SC coupling beam. Compared with the fat cyclic responses of the conventional steel coupling beam with greater energy dissipation (Fig. 7), the proposed SC coupling beam can also provide sufficient energy dissipation. More importantly, the majority of the inelastic damages of this novel SC coupling beam are concentrated in the steel angles, which can be easily and rapidly inspected/replaced after earthquakes without operation.

SC capability was evaluated by the ratio of recovered rotation to the peak rotation in each loading cycle. As shown in Fig. 10(b), the SC coupling beam showed a very high recovery ratio with excellent SC capability. The lowest recovery ratio of 81% at 0.02 rad rotation has attained. However, the recovery ratio increased and was up to 90% at 0.08-rad loading. Excellent SC capability indicates that the SC coupling beam has a good prospect in the earthquake resilient design.

To analyze the influence of the steel angles on the seismic performance of the SC coupling beam, the equivalent viscous damping ratio ζ_{eq} was calculated, which is expressed by $\zeta_{eq} = E_D/(4\pi E_S)$, where E_D is the total energy dissipated per cycle, and E_S is the elastic strain energy at peak amplitude. Fig. 10(c) shows the variation of the equivalent viscous damping ratios with increasing amplitude. The SC coupling beam exhibited a high energy dissipation (ζ_{eq} = 17.1% at 8% rotation). ACI [27] uses the relative ED ratio β_h to evaluate the energy dissipation, which stipulates the relative energy dissipation ratio should not be less than 0.125 at a design target amplitude, which can be estimated as the equivalent viscous damping ratio by ζ_{eq} =

$2\beta_h/\pi$. It shows that the SC coupling beam can satisfy the requirement of the energy dissipation, which again confirms the favorable role of the steel angles in enhancing the energy dissipation of the proposed SC coupling beam system.

The average axial strains of two SMA bolts (SMA-1 and SMA-2 are the outmost and inner side bolts in the left bottom, respectively) are shown in Fig. 10(d). As expected, SMA bolts are subjected only to tensile force during the entire loading process. This design can avoid the buckling of SMA bolt. The maximum strain of the SMA-1 was 5.4% at the 0.08-rad loading, which is smaller than the predefined strain value (i.e., 6%) due to the elastic deformation of the coupling beam not considered in the initial estimate. For SMA-2, the SMA bolt keeps tightening after the lateral force is removed completely.

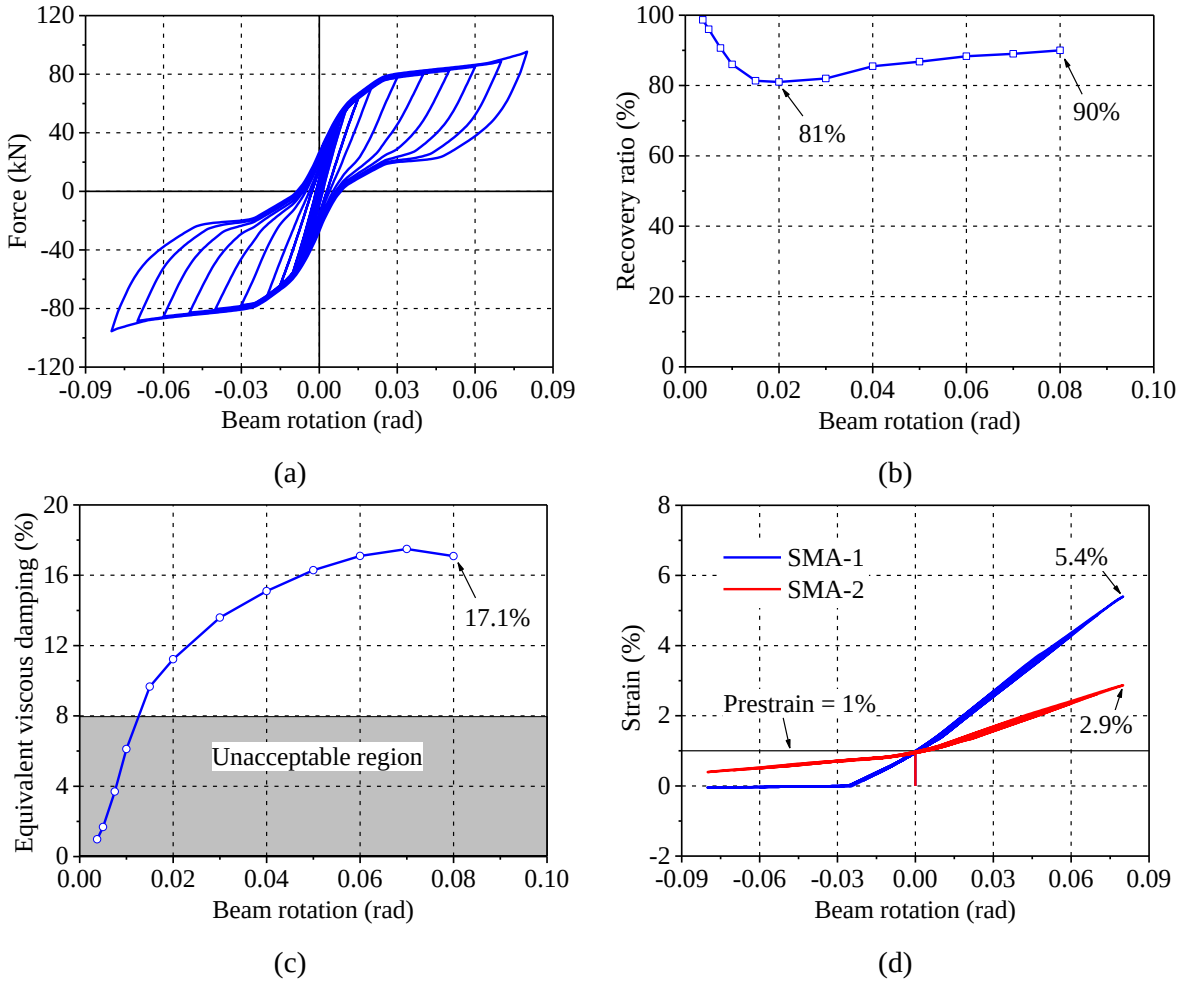

Fig. 10 – Performance evaluation of the SC coupling beam: (a) force–beam rotation hysteresis loops, (b) SC capability, (c) energy dissipation, and (d) strain–beam rotation relationships of the SMA bolts.

5. Conclusions

This paper proposes a novel SC steel coupling beam designed with SMA bolts and steel angles. The novel SC coupling beam is composed of two elastic beam segments and one rocking segment. Elastic beam segment is designed by the steel beam that connects to the RC walls at both ends of the coupling beam, whereas the rocking segment located in the middle of the coupling beam is controlled by the SMA bolts and steel angles. The shear key and the groove are designed with inclined surfaces, which help to accommodate the rotation flexibility of the rocking segment and then eliminate the beam elongation effect under cyclic

loading. The design philosophy assumes that all inelastic deformations will be concentrated in the SMA bolts and steel angles, which will be accommodated through the rocking behavior at the interfaces between the elastic and rocking segments.

The SC coupling beam exhibited excellent flag-shaped responses compared with the typical hysteretic curves of conventional RC or steel coupling beam. Excellent SC capability indicates that the SC coupling beam has a good prospect in the earthquake resilient design. Due to the additional steel angles, the SC coupling beam can satisfy the requirement of the energy dissipation, which again confirms the favorable role of the steel angles in enhancing the energy dissipation of the proposed coupling beam system. The specimen exhibited the expected deformed shapes under cyclic loading, where the ingeniously designed shear keys can accommodate the rotation flexibility of the rocking segment, and thus eliminate the beam elongation effect under cyclic loading.

From the design perspective, designers can cater to different performance objectives by flexibly adjusting the dimensions of the SMA bolts and steel angles. Therefore, the proposed SC coupling beam will provide a promising solution for high-performance seismic-resisting structural systems that are suitable for resilient and sustainable civil infrastructure.

6. Acknowledgements

The authors are grateful for the financial support from the Grand-in-Aid for Scientific Research (JSPS KAKENHI Grant No. JP 19F19077). The findings and opinions expressed in this paper are solely those of the authors and not represent the views of the sponsor.

7. References

[1] ACI (American Concrete Institute) (2019): Building Code Requirements for Structural Concrete (ACI 318-19) and Commentary on Building Code Requirements for Structural Concrete (ACI 318R-19). ACI Committee 318, Farmington Hills, MI

[2] Ministry of Housing and Urban-Rural Development of the People's Republic of China (MOHURD) (2014): Code for Seismic Design of Buildings (GB 50011-2010). China Architecture and Building Press, Beijing, China.

[3] Wyllie LA (1992): Analysis of the collapsed Armenian precast concrete frame buildings. In Earthquake Engineering, *Proc. 10th World Conference on Earthquake Engineering*, Balkema, Rotterdam, 63-66.

[4] Wang YY (2008): Lessons learned from the "5.12" Wenchuan Earthquake: evaluation of earthquake performance objectives and the importance of seismic conceptual design principles. *Earthquake engineering and engineering vibration*, **7**(3), 255-262.

[5] Fortney PJ, Shahrooz BM, Rassati GA (2007): Large-scale testing of a replaceable "fuse" steel coupling beam. *Journal of structural engineering*, **133**(12), 1801-1807.

[6] Shahrooz BM, Fortney PJ, Harries KA (2018): Steel coupling beams with a replaceable fuse. *Journal of Structural Engineering*, **144**(2), 04017210.

[7] Chung HS, Moon BW, Lee SK, Park JH, Min KW (2009): Seismic performance of friction dampers using flexure of RC shear wall system. *The Structural Design of Tall and Special Buildings*, **18**(7), 807-822.

[8] Lu XL, Chen Y, Jiang HJ (2018): Earthquake resilience of reinforced concrete structural walls with replaceable "fuses". *Journal of Earthquake Engineering*, **22**(5), 801-825.

[9] Ji XD, Wang, YD, Ma QF, Okazaki T (2017): Cyclic behavior of replaceable steel coupling beams. *Journal of Structural Engineering*, **143**(2), 04016169.

[10] Mansour N, Christopoulos C, Tremblay R (2011): Experimental validation of replaceable shear links for eccentrically braced steel frames. *Journal of Structural Engineering*, **137**(10), 1141-1152.

[11] Weldon BD, Kurama YC (2010): Experimental evaluation of posttensioned precast concrete coupling beams. *Journal of Structural Engineering*, **136**(9), 1066-1077.

[12] Kurama YC, Weldon BD, Shen Q (2006): Experimental evaluation of posttensioned hybrid coupled wall subassemblages. *Journal of Structural Engineering*, **132**(7), 1017-1029.

[13] DesRoches R, McCormick J, Delemont M (2004): Cyclic properties of superelastic shape memory alloy wires and bars. *Journal of Structural Engineering*, **130**(1), 38-46.

[14] Saiidi MS, Wang HY. (2006): Exploratory study of seismic response of concrete columns with shape memory alloys reinforcement. *ACI Structural Journal*, **103**, 436-443.

[15] Zhu SY, Zhang YF (2007): Seismic behaviour of self-centring braced frame buildings with reusable hysteretic damping brace. *Earthquake engineering & structural dynamics*, **36**(10), 1329-1346.

[16] Zhu SY, Zhang YF (2008): Seismic analysis of concentrically braced frame systems with self-centering friction damping braces. *Journal of Structural Engineering*, **134**(1), 121-131.

[17] Qiu CX, Zhu SY (2017): Shake table test and numerical study of self-centering steel frame with SMA braces. *Earthquake Engineering & Structural Dynamics*, **46**(1), 117-137.

[18] Wang B, Zhu SY (2018): Superelastic SMA U-shaped dampers with self-centering functions. *Smart materials and structures*, **27**(5), 055003.

[19] Wang B, Zhu SY (2018): Cyclic tension–compression behavior of superelastic shape memory alloy bars with buckling-restrained devices. *Construction and Building Materials*, **186**, 103-113.

[20] Wang B, Zhu SY, Zhao JX, Jiang HJ (2019). Earthquake resilient RC walls using shape memory alloy bars and replaceable energy dissipating devices. *Smart Materials and Structures*, **28**(6), 065021.

[21] Wang B, Zhu SY, Qiu CX, Jin H (2019): High-performance self-centering steel columns with shape memory alloy bolts: design procedure and experimental evaluation. *Engineering Structures*, **182**, 446-458.

[22] Mao CX, Wang ZY, Zhang LQ, Li H, Ou JP (2012): Seismic performance of RC frame-shear wall structure with novel shape memory alloy dampers in coupling beams. *Proc. 15th World Conference on Earthquake Engineering*, Lisbon, Portugal. Paper No. 4988.

[23] Xu X, Tu JQ, Cheng GM, Zheng JH, Luo YZ (2019): Experimental study on self-centering link beams using post-tensioned steel-SMA composite tendons. *Journal of Constructional Steel Research*, **155**, 121-128.

[24] Garlock MM, Ricles JM, Sause R (2003): Cyclic load tests and analysis of bolted top-and-seat angle connections. *Journal of Structural Engineering*, **129**(12), 1615-1625.

[25] Lu XZ, Zhang L, Cui Y, Li Y, Ye LP (2018): Experimental and theoretical study on a novel dual-functional replaceable stiffening angle steel component. *Soil Dynamics and Earthquake Engineering*, **114**, 378-91

[26] AISC (American Institute of Steel Construction) (2016): Seismic provisions for structural steel buildings. ANSI/AISC 341-16, Chicago, Illinois, US.

[27] ACI (American Concrete Institute) (2008): Acceptance criteria for special unbonded post-tensioned precast structural walls based on validation testing. ACI ITG-5.1-07, Farmington Hills, MI.

